Dissolution modes of Fe/Cu and Cu/Fe deposits

S. Delage, B. Legrand, and F. Soisson
SRMP-DECM, CEA Saclay, 91191 Gif-sur-Yvette Cedex, France

A. Saúl
CRMC2-CNRS, Campus de Luminy, Case 913, 13288 Marseille Cedex 9, France
(Received 28 October 1997; revised manuscript received 10 July 1998)

Using a kinetic model that includes bulk and surface driving forces, we study the different modes occurring during the kinetics of dissolution of thin (1 or 2 ML) and thick (10 ML) deposits of Cu on Fe and Fe on Cu. For a thin deposit, due to the lower surface energy of Cu, the dissolution kinetics is slower for the Cu on Fe case than for Fe on Cu. In the first case the Cu remains at the surface up to the total dissolution. For the inverse deposit a surfactant effect takes place where the deposit is buried by one or two planes of the substrate element. Before the total dissolution and depending on the temperature and the deposit thickness the kinetics can slow down due to the appearance of quasistationary configurations that corresponds to equilibrium solutions of an equivalent finite system having the same instantaneous quantity of matter. For a thick deposit of Cu on Fe the deposit also remains at the surface and the dissolution takes place following a layer by layer dissolution mode, which corresponds to the successive dissolution of each precipitate plane, starting from the plane at the interface between the deposit and the substrate. The shape of this interface corresponds to the equilibrium interface between two semi-infinite phases having the bulk solubility limit concentrations. For the inverse deposit, first a surfactant effect occurs, leading to a copper bilayer floating on the surface. Then, two layer by layer dissolution modes take place, which correspond to the dissolution either from the bottom or from the top of the precipitate. These layer by layer dissolution modes are linked to the large miscibility gap of the phase diagram. We use a ''local equilibrium'' concept that allows us to compare all the configurations obtained during the kinetics of dissolution to concentration profiles of ''stable'' or ''metastable'' solutions of related equilibrium situations. [S0163-1829(98)04147-2]

I. INTRODUCTION

The structure and features of epitaxially grown ultrathin films have drawn much attention since the development of new magnetic materials.[1–3] In some cases, it has become possible to stabilize new metastable structures near the surface, which exhibit magnetic properties that differ from the bulk ones. The problem is, of course, more general and concerns not only magnetic materials but also other metallic alloys presenting interesting properties (reactivity for catalysis, for example) that depend on their surface structure and composition. The general problem is very complicated and can depend on many factors: the chemical properties of the binary system, the temperature, the deposit thickness, the quality of the substrate surface, the surface orientation, etc. Moreover, if the deposition is made at a temperature at which the interdiffusion is also active, the structures obtained will also depend on the deposition flux.

The study of the dissolution modes, i.e., the different ways a perfect *A* deposit dissolves on a semi-infinite *B* substrate at a given temperature, can teach us about the importance of at least three important factors: the chemical properties (the tendency of the binary system to order or to phase separate, and the difference between surface energies), the temperature, and the deposit thickness. In systems with ordering tendency (CuPd,PtSn, . . .), recent studies[4,5] have shown the stabilization at the surface of quasistationary structures that do not exist in the bulk (surface alloys) that precedes the total dissolution of the deposit. The time that these surface alloys remain near the surface, their sequence of apparition, and their spatial extension can depend strongly on the temperature and on the difference in surface energy between the deposit and the substrate. For systems with phase separation tendency, before the ineluctable total dissolution, the deposited *A* atoms will try to form clusters or layers in order to minimize the number of heteroatomic neighbors. These clusters or layers can either remain at the surface or be embedded by substrate *B* layers depending on the sign of the difference in surface energy.

The aim of this paper is the study of the dissolution modes for systems with a phase separation tendency, as a function of the deposit thickness, the temperature, and the sign of the difference in surface energy (dissolution of *A* in *B* or *B* in *A*). The results presented here concern the FeCu system, but can also be applied to other systems that present a tendency to phase separation and a strong surface segregation (NiAg, CuAg, AuNi, CoAu, AgRh, . . .). We will show that the different dissolution modes are indeed mainly due to these two features. Many experimental studies were devoted to the understanding of the growth mode of Fe thin films deposited on Cu, especially at low temperature in order to avoid interdiffusion. However, this interdiffusion takes place even at room temperature, the strong surface segregation of copper being at the origin of such behavior.[6–8]

The theoretical model used here takes into account the bulk driving forces for phase separation, and the driving forces for surface segregation as well. The study was made on the bcc crystallographic structure and the compact (110)

surface orientation. We are aware that, in the temperature range that we consider, the iron is bcc but the copper is fcc. Nevertheless, we think that the main results presented here do not depend strongly on the structure, because some of these results were obtained similarly for the NiAg system[9] (both metals are fcc).

This paper is organized as follows. In Sec. II, we give a brief description of the theoretical model used. Section III presents the results of the kinetics, in Sec. III A for Cu deposited on Fe, and in Sec. III B for Fe deposited on Cu. Finally, in Sec. IV, we analyze the physical origin of the various dissolution modes obtained during the kinetics via a ''local equilibrium'' concept.

II. ENERGETIC AND KINETIC MODELS

Our simulations are based on an energetic model, the tight-binding Ising model (TBIM),[10] the energetic parameters of which come from a tight-binding description of the electronic structure. It had been originally developed to study equilibrium surface segregation in transition- and noble-metal alloys. The kinetic extension of the TBIM is the kinetic tight-binding Ising model (KTBIM) that is a simple one-dimensional mean-field model.[11,12] It assumes homogeneous concentrations per plane parallel to the surface and ensures that the steady-state concentration profile corresponds to the same one given by the TBIM.

In the KTBIM framework, the time dependence of the mean concentrations $c_i(t)$ per plane parallel to the surface are calculated as a detailed balance between incoming and outgoing fluxes:

$$\frac{\partial c_0}{\partial t}=\frac{Z_1' D}{a^2}\left[(1-c_0)\frac{c_1}{\gamma_0}-c_0\gamma_0(1-c_1)\right],$$

$$\frac{\partial c_i}{\partial t}=\frac{Z_1' D}{a^2}\left[(1-c_i)\left\{\gamma_{i-1}c_{i-1}+\frac{c_{i+1}}{\gamma_i}\right\}-c_i\left\{\frac{(1-c_{i-1})}{\gamma_{i-1}}+\gamma_i(1-c_{i+1})\right\}\right],\quad i>0, \tag{1}$$

where $i=0$ is the surface plane, $a=2.86$ Å is the lattice parameter, Z_1' the number of first neighbors of a site in the adjacent planes, and $D=D_0\exp(-Q/kT)$ the bulk diffusion coefficient,[13] with $D_0=300$ cm^2/s and $Q=2.94$ eV/at for diffusion of Cu impurities in Fe.[14]

For an A_cB_{1-c} alloy if $c_i(t)$ is the instantaneous concentration of A in plane i, $\gamma_i(t)$ is related to the instantaneous transition probability to exchange an A atom in plane i with a B atom in plane $i+1$. In the KTBIM model, $\gamma_i(t)$ depends on the instantaneous segregation energies $\Delta H_i(t)$ as follows:

$$\gamma_i(t)=\exp\left(\frac{\Delta H_i(t)-\Delta H_{i+1}(t)}{2kT}\right), \tag{2}$$

where $\Delta H_i(t)$ is the energy needed to exchange a B atom in the plane i with an A atom from the bulk. Then, the difference appearing in Eq. (2): $\Delta H_i(t)-\Delta H_{i+1}(t)$ is the energy needed to exchange a B atom from plane i with an A atom from plane $i+1$.

The coherence between the kinetic (KTBIM) and the equilibrium model (TBIM) appears at this point because we write the instantaneous segregation energies as the sum of three terms[10] as in the equilibrium model:

$$\Delta H_i=\Delta h_i+\Delta h_i^{\text{size}}+\Delta H_i^{\text{alloy}}. \tag{3}$$

We will briefly summarize the significance of these three terms and their relative importance for the FeCu system:

(i) Δh_i is related to the difference in surface energy and it is generally different from zero only for the surface plane ($i=0$). The difference in surface energy between Fe and Cu for the (110) face in the bcc structure favors a strong copper segregation: $\Delta h_0=\tau_{Cu}-\tau_{Fe}=-0.272$ eV/at.[15]

(ii) Δh_i^{size} accounts for the contribution to the segregation energy due to the difference in size of the alloy constituents,[16] it is also generally significative only for the surface and first underlayer planes. The size mismatch between Cu and Fe is very small, less than 1%, and Δh_i^{size} can be neglected.

(iii) $\Delta H_i^{\text{alloy}}$ is the alloying effect:

$$\Delta H_0^{\text{alloy}}=\sum_{j=1,2}V_j[Z_j'+2Z_j(c_0-c)+2Z_j'(c_1-2c)] \tag{4}$$

and

$$\Delta H_i^{\text{alloy}}=\sum_{j=1,2}2V_j[Z_j(c_i-c)+Z_j'(c_{i-1}+c_{i+1}-2c)],\quad i>0, \tag{5}$$

Z_j and Z_j' are the number of nearest ($j=1$) and next-nearest ($j=2$) neighbors in the same plane and in the adjacent planes (below or above), respectively. For the bcc(110) orientation all these neighbors are located in the same plane or in the adjacent planes and $Z_1=4$, $Z_1'=2$, $Z_2=2$, $Z_2'=2$. c is the bulk concentration and let us note that we have chosen to work always in concentration of the minority element, i.e., c and c_i represent the concentration of Cu when studying dissolution of Cu on Fe, and the concentration of Fe in the Fe on Cu case. V_1 and V_2 are the effective pair interactions between nearest and next-nearest neighbors:

$$V_j=\frac{1}{2}(V_j^{FeFe}+V_j^{CuCu}-2V_j^{FeCu}),\quad j=1,2. \tag{6}$$

They characterize the bulk tendency to order or to phase separate ($V<0$, accounts for tendency to phase separation). For the bcc structure, the atomic interaction parameters decrease in such a way that V_2 is roughly equal to $V_1/2$.[17] We have used this relation and the value $V_1=-0.036$ eV/at to reproduce the experimental solubility limit.[13]

The system (1) is worked for a finite number N of equations using adimensional time $\tilde{t}=t/t_0$, where $t_0=Z_1'D/a^2$. For the dissolution kinetics of M monolayers of A on B the initial conditions are $c_i(t=0)=1$, $i=0$, $M-1$ and $c_i(t=0)=0$, $i=M$, $N-1$. The boundary condition $c_N(t)=0$ represents the contact with a pure B bulk. To integrate the set of Eqs. (1) we use a fourth-order Runge-Kutta algorithm.[18]

A large number of equations is *a priori* needed in order to get a dynamics independent of the system size. In order to

minimize the number of equations, we take advantage that far from the surface region (typically 50 planes) the concentrations are very low $c_i \ll 1$ and the nonlinear system of Eqs. (1) can be approximated by the discrete classical Fick's equation :

$$\frac{\partial c_i}{\partial t} = \frac{D}{d^2}(c_{i+1} + c_{i-1} - 2c_i), \tag{7}$$

where $d = a/Z_1'$ is the interplane distance. We can then modify the discretization of Eqs. (7):

$$\frac{\partial c_i}{\partial t} = \frac{2D}{d_i + d_{i-1}}\left(\frac{c_{i-1} - c_i}{d_{i-1}} + \frac{c_{i+1} - c_i}{d_i}\right) \tag{8}$$

and use, for example, a monotonically increasing distance $d_i = 1.2 d_{i-1}$ for $i \geqslant 50$.[19] It allows us to typically decrease the number of equations from 10 000 to 100.

III. RESULTS

In this section we present the results of dissolution kinetics for deposits of Cu on Fe and of Fe on Cu. In both cases we will show results for thin (1 or 2 ML) and thick (10 ML) deposits. We will present results for only one temperature ($T = 1100$ K), or two temperatures ($T = 700$ K and $T = 1100$ K) when an appreciable qualitative difference in function of the temperature occurs.

In the Cu on Fe case the element of lower surface energy is already in the surface and the dissolution modes are simpler than in the inverse case.

The dissolution of Fe deposited on Cu shows a completely different behavior because the element of higher surface energy is now initially on top. We will show in the following that this feature leads to a new behavior for both the thin (1 and 2 ML) and thick (10 ML) dissolution kinetics. We will first study the thin deposit case at low temperature, 700 K, and high temperature, 1100 K, and then the thick deposit one only at 1100 K.

The bulk solubility limits within the mean-field approximation are $c_\alpha = 0.0014$ and 0.017 at $T = 700$ K and $T = 1100$ K, respectively.

A. Cu deposited on Fe

1. 1 ML of Cu on Fe(110)

We consider here the dissolution kinetics of one monolayer of Cu deposited on a Fe (110) substrate. In Fig. 1, we report the copper concentration of the surface c_0 and first underlayer c_1 planes as a function of $\sqrt{t/t_0}$. We clearly observe a linear behavior of the surface concentration c_0 with $\sqrt{t/t_0}$ in the major part of the kinetics. During the dissolution of Ag deposited on Cu(111), which is similar in many aspects with the dissolution of Cu on Fe(110) (the bulk clustering tendency and strong tendency to surface segregate for the deposited element), Auger electron spectroscopy experiments[20,21] show a similar behavior for the evolution of the Ag concentration.

This linear behavior with $\sqrt{t}$ is known to happen experimentally in cases of strong segregation. It can be found theoretically as the approximate solution of the KTBIM equations as follows. First, we assume that the concentration c_k of the k plane under the surface remains constant during the dissolution. Second, if $c_k \ll 1$ the system of Eqs. (1) for the region $i \geqslant k$ can be reasonably well approximated by the Fick's equation. Then the analytical solution of the concentration profile for this region $c_i(t) = c_k \mathrm{erfc}[(i-k)\sqrt{t_0/4t}]$ allows us to estimate the flux of matter coming from the surface $j_0(t) = c_k/\sqrt{\pi t t_0}$ and consequently the decrease of the copper concentration at the surface:[20,22]

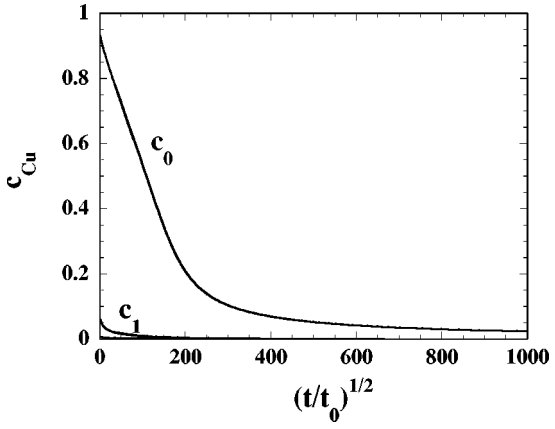

FIG. 1. Kinetics of dissolution of one Cu monolayer on Fe(110) at $T = 1100$ K. The surface and first underlayer Cu concentrations $c_0(t)$ and $c_1(t)$ are plotted vs $\sqrt{t/t_0}$.

$$c_0(t) \approx c_0(0) - 2c_k\sqrt{\frac{t}{\pi t_0}}. \tag{9}$$

We will show in Sec. IV A that $c_2(t)$ remains constant during the dissolution due to the local equilibrium. Equation (9) with the constant value of c_2 gives a slope of $c_0(t)$ as a function of $\sqrt{t}$ that differs only 15% of the one from Fig. 1. Let us add that the role of the temperature is essentially to change the slope value.

2. 10 ML of Cu on Fe(110)

The dissolution kinetics of 10 ML of Cu on Fe is shown in Fig. 2. The deposit undergoes a layer by layer dissolution

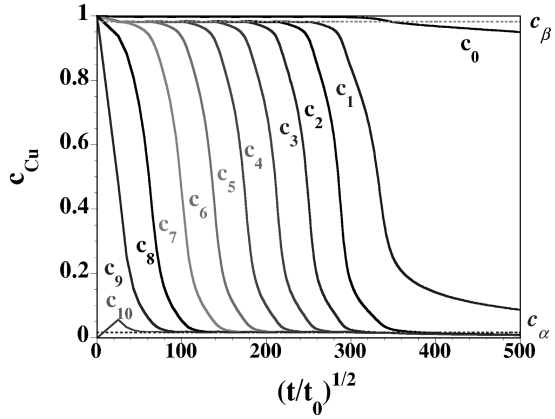

FIG. 2. Kinetics of dissolution of 10 ML of Cu on Fe(110) at $T = 1100$ K. The Cu concentration of the 11 planes near the surface $[c_i(t),\ i = 0,10]$ is plotted vs $\sqrt{t/t_0}$. c_α and c_β are the bulk solubility limits (dotted lines).

starting from the plane at the interface between the deposit and the substrate.[23] Each deposit plane initially pure in copper reaches rapidly the solubility limit c_β (the Cu-rich one), then the copper atoms leave each deposit plane successively, the concentrations of these planes decreasing rapidly to c_α (the solubility limit of the Fe-rich phase). It leads to a c_α/c_β interface that moves towards the surface. We can see that the planes 8 to 2 show exactly the same behavior spaced out from a constant value in $\sqrt{t}$. Moreover, the dissolution of these planes takes place while the concentrations of the planes below remain constant at a value close to c_α.

We can use the same argument than above assuming that the concentration of some plane below the deposit remains constant during the dissolution to find that the total quantity of copper $m(t)$ must decrease as

$$m(t)=\sum_{i=0}^{M-1} c_i(t)\approx M-2c_\alpha\sqrt{\frac{t}{\pi t_0}}, \tag{10}$$

where N is the total number of Cu planes initially deposited.[24] Then, the delay between the dissolution of two successive planes can be estimated: $\Delta(\sqrt{t/t_0})=\sqrt{\pi}/(2c_\alpha)\approx 52$, in good agreement with the spacing shown in Fig. 2. In the last stage of the dissolution ($\sqrt{t/t_0}>350$), the segregation effect tends to slow down the dissolution of the last two planes.

At lower temperatures the same layer by layer dissolution mode is observed but a lower solubility limit {c_α decreases as $\exp[(Z_1V_1+Z_2V_2)/kT]$ at low temperature} can significantly slow down the process. Another effect due to the temperature is that the instantaneous c_α/c_β interface that moves to the surface becomes more abrupt at lower temperatures.

Finally, let us mention that the standard diffusion theory based on Fick's description cannot give the same results as the KTBIM model.[23] In Fick's description the flux of matter is proportional to the concentration gradient, all the planes will then react together in order to minimize this gradient and they will dissolve almost simultaneously.

B. Fe deposited on Cu

1. 1 and 2 ML of Fe on Cu(110)

$T=700$ *K*. The Fe concentration of the five layers close to the surface vs the square root of time for the dissolution of 1 ML of Fe on Cu(110) is shown Fig. 3. In a first time, the strong copper segregation leads to an immediate surface enrichment in copper [$c_0(t)$ decrease rapidly from 1 to 0]. This rapid enrichment takes place via atom exchanges between the first two planes, the planes labeled 2 and 3 playing only a minor role. Then the plane labeled 1 enriches in copper, whereas the iron atoms spread between planes 2 and 3, forming a mixed bilayer. These planes have almost the same concentration, and we call this situation configuration (c_2,c_3). We introduce here a notation that will be useful in the following: when most of the precipitate is located in the two consecutive planes k and $k+1$ we will call it configuration (c_k,c_{k+1}). This (c_2,c_3) configuration takes place for $\sqrt{t/t_0}$ from 5 to 12 and after this time it leads to a Fickian dissolution of all the planes under the surface (the surface being always pure copper). That is what we call the surfactant dissolution mode, the deposited element dissolves while it is buried below one or two monolayers of the substrate.

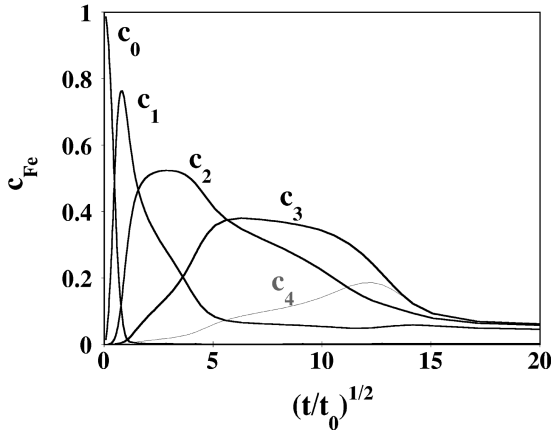

FIG. 3. Kinetics of dissolution of one Fe monolayer on Cu(110) at $T=700$ K. The Fe concentration of the five planes near the surface [$c_i(t)$, $i=0,4$] is plotted vs $\sqrt{t/t_0}$.

For the dissolution of 2 ML of Fe on Cu(110), the kinetics is more complicated (see Fig. 4). First ($\sqrt{t/t_0}<4$), the surface plane enriches in copper, leading to the appearance of a copper monolayer floating on the deposit, i.e., the Fe concen-

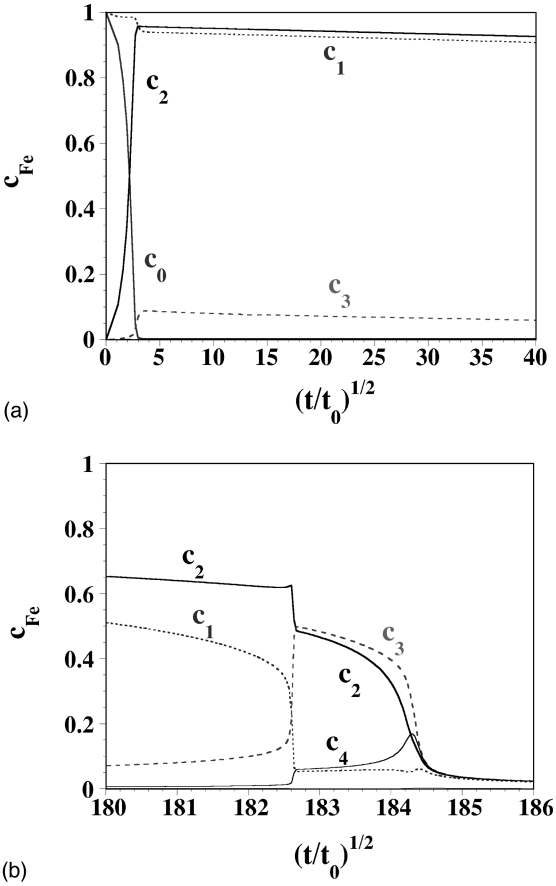

FIG. 4. Kinetics of dissolution of two Fe monolayers on Cu(110) at $T=700$ K. (a) Fe concentration of the four planes near the surface [$c_i(t)$, $i=0,3$] vs $\sqrt{t/t_0}$ at the beginning of the dissolution kinetics, (b) Fe concentration of the five planes near the surface [$c_i(t)$, $i=0,4$] vs $\sqrt{t/t_0}$ at longer time.

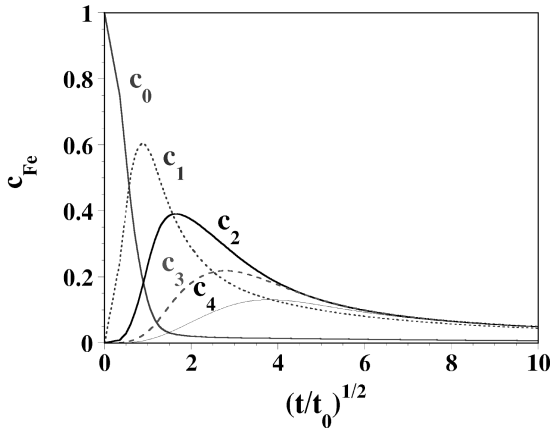

FIG. 5. Kinetics of dissolution of one Fe monolayer on Cu(110) at $T=1100$ K. Fe concentration of the five planes near the surface $[c_i(t),\ i=0,4]$ vs $\sqrt{t/t_0}$.

tration of the first three planes is $c_0 \simeq 0$, $c_1 \simeq 1$, and $c_2 \simeq 1$ as can be seen in Fig. 4(a). This situation of a Cu monolayer floating above two mixed planes, a (c_1,c_2) configuration, corresponds to a quasistationary solution of the system of equations (1) that slow down significatively the kinetics. That is the reason why we have only presented the first part of the kinetics in Fig. 4(a) and a zoom at a longer time in Fig. 4(b). For the part of the kinetics not shown ($\sqrt{t/t_0}$ between 40 and 180) the Fe concentration of the planes labeled 1 and 2 decrease slowly and monotonously. Then the Fe concentration of the first layer under the surface (c_1) suddenly decreases and a new configuration formed by a floating Cu bilayer above two mixed planes takes place. This (c_2,c_3) configuration then disappears for $\sqrt{t/t_0} > 184$ giving rise to a Fickian dissolution for all the planes except for the surface plane, which is always pure Cu as in the end of kinetics of the 1 ML Fe on Cu case. We will see in Sec. IV how we can link these quasistationary (c_k,c_{k+1}) configurations to metastable solutions of the equilibrium equations describing the segregation in FeCu thin films.

$T=1100$ *K.* The same study at 1100 K is shown in Fig. 5 for 1 Fe monolayer deposit on Cu(110) and in Fig. 6 for 2 Fe ML. For 1 ML, the beginning of the kinetics is similar to the one at 700 K (Fig. 3). The Fe surface concentration decreases rapidly and reaches nearly zero at $\sqrt{t/t_0}=2$. This copper enrichment of the surface plane occurs via atom exchanges between the first three planes (see the increase of the Fe concentration of c_1 and c_2 while c_0 decreases). Then, c_1 decreases its Fe content at the expense of the planes below, they finally dissolve via a classic Fickian dissolution type. We do not observe at this temperature a (c_2,c_3) configuration corresponding to the precipitate located in the planes 2 and 3 as we have seen at 700 K.

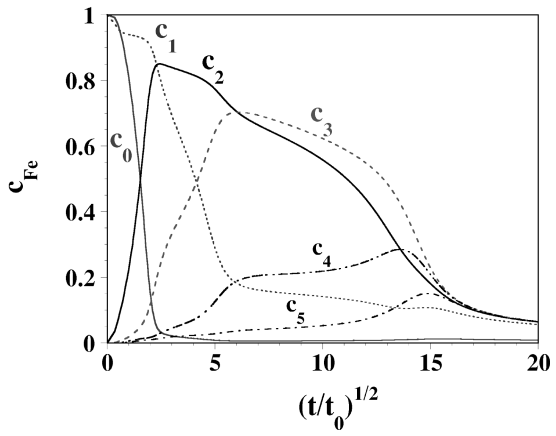

FIG. 6. Kinetics of dissolution of two Fe monolayers on Cu(110) at $T=1100$ K. Fe concentration of the six planes near the surface $[c_i(t),\ i=0,5]$ vs $\sqrt{t/t_0}$.

For the dissolution of 2 ML of Fe on Cu there are also differences at 1100 K with respect to the 700 K case. At 700 K we have found the appearance of a (c_1,c_2) configuration followed by a (c_2,c_3) one. At 1100 K only the second quasistationary configuration appears (see Fig. 6). Let us compare this kinetics to the one at 700 K in Fig. 4. First, the usual rapid copper enrichment at the surface takes place as at lower temperature. However the (c_1,c_2) metastable configuration does not appear, the c_2 concentration increases while c_1 remains constant and then this concentration decreases at the expense of c_3. Next, a (c_2,c_3) configuration occurs, starting with concentrations $c_2 \simeq c_3 \simeq 0.7$, and decreasing slowly with time. At $T=700$ K, the (c_2,c_3) configuration started from lower concentrations $c_2 \simeq c_3 \simeq 0.5$, the difference between the two cases is the previous stage of the dissolution.

Moreover, let us compare the time scale of the c_0 decrease in the case of 1 ML Cu/Fe (Fig. 1) and 1 ML Fe/Cu (Fig. 5) kinetics at $T=1100$ K. In Fig. 1, the surface concentration of copper reaches 0.1 when $\sqrt{t/t_0} \simeq 200$. In the case of 1 ML Fe/Cu deposit, the decrease of the surface concentration in iron is very fast, and c_0 almost vanishes at $\sqrt{t/t_0}=2$. This difference points out the strong segregation effect, which leads either to a trapping of copper at the surface for 1 ML Cu/Fe deposit, or to a fast enrichment of copper at the surface in the case of a 1 ML or 2 ML Fe/Cu deposit.

2. 10 ML of Fe on Cu(110)

In the case of a thick deposit of Fe on Cu, we can expect a competition of two behaviors described before. First, because the element of highest surface energy is now on top, we can wonder if the surface segregation effect, which leads to the surfactant effect for 1 and 2 ML Fe/Cu, would be strong enough to allow the climb of the copper atoms through the deposit. Second, as in the case of the dissolution kinetics of thick deposits of Cu on Fe, we can expect to obtain the particular layer by layer dissolution mode that is controlled by the immiscibility of the constituents.

In Fig. 7(a) we show the dissolution kinetics of 10 ML of Fe deposited on Cu at $T=1100$ K. We schematize the main features of the kinetic evolution in Fig. 7(b). We can see that in spite of the deposit thickness, the strong segregation leads to a rapid Cu enrichment of the surface, the deposit being buried under the surface. This surfactant effect occurs via effective atom exchanges between the plane 0 and the plane 10, which was the first pure copper plane under the deposit. At this stage of the dissolution [labeled II in Fig. 7(b)], there is no loss of iron matter in the substrate. Then a competition between two types of layer by layer dissolution modes takes

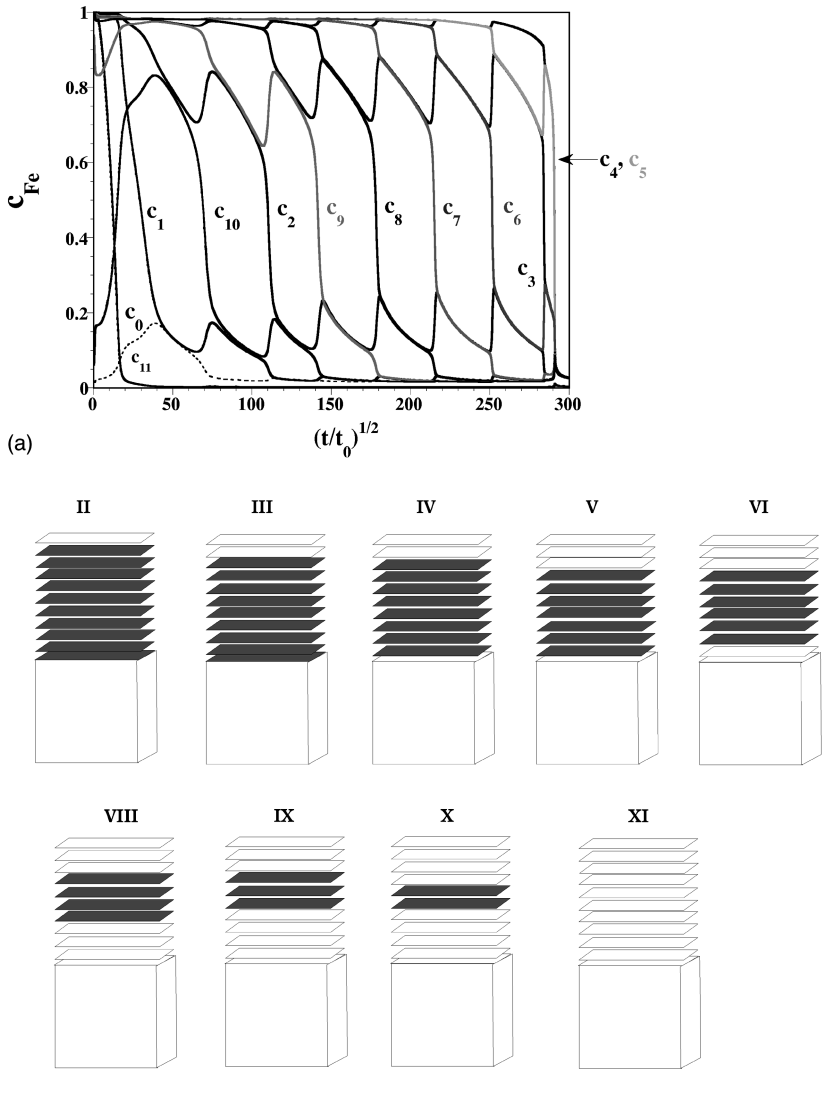

FIG. 7. Kinetics of dissolution of 10 ML of Fe on Cu(110) at $T=1100$ K. (a) Fe concentration of the 12 planes near the surface $[c_i(t),\ i=0,11]$ vs $\sqrt{t/t_0}$. (b) Schematic representation of the deposit evolution.

place: a new one from above and the other from the bottom of the deposit. The first one to happen is from above (labeled III) because, for energetic reasons, the Fe precipitate prefers to move away from the surface, i.e., the c_α/c_β interface is more constrained close to the surface than in the bulk The next two are from the bottom (IV) and from above (V) and finally from stages VI–IX, a layer by layer mode from the bottom takes place, as in the 10 ML Cu/Fe case.

IV. LOCAL EQUILIBRIUM

We have seen in the preceding sections that the dissolution of a deposit on a substrate can give rise to the appearance of quasistationary configurations that slow down the dissolution significantly. In this section we will show how these configurations can be linked to ''stable'' or ''metastable'' solutions of *related equilibrium situations*.

The idea was first introduced, to our knowledge, by Lagües and Domange[25] to study dissolution and segregation kinetics in cases of strong segregation. They have suggested that because of the strong segregation the near surface kinetics is faster than the bulk diffusion, and we can then expect the appearance of a local equilibrium in the surface selvedge.[25] Thus, for example, the dissolution kinetics of a very thin deposit can be linked to the equilibrium segregation isotherm.[20] This idea can be generalized to cases where there is somewhere a more rapid diffusion establishing a local equilibrium situation in comparison with the diffusion phenomena settling the global thermodynamic equilibrium. As we will show below this is also so for the dissolution of a thick deposit during the layer by layer dissolution mode where a local equilibrium also occurs. In this case the *related equilibrium situation* is the metastable equilibrium interface of the deposit confined in a finite region close to the surface but in contact with the volume.

The idea is therefore to compare the kinetics obtained using the KTBIM to the equilibrium profiles of this *related equilibrium situations*. The different choice of these equilibrium situations allows us to define two different ways of representing the local equilibrium.

First local equilibrium representation (LE_1): In this case the *related equilibrium situations* are the isotherm equilibrium segregation profiles as a function of the bulk concentration c. To calculate the equilibrium profile of a semi-infinite binary alloy, we must minimize the total free energy of the system G_{TBIM} with respect to the layer concentrations c_i, which gives the following nonlinear coupled system of equations:[26]

$$\frac{c_i}{1-c_i}=\frac{c}{1-c}\exp\left\{-\frac{\Delta H_i(c_{i-1},c_i,c_{i+1},c)}{kT}\right\}. \quad (11)$$

It is easy to see that the steady-state concentration profile of the kinetics equations [Eq. (1)] is solution of this system of equations. The equilibrium profile [$c_0(c)$, $c_1(c)$, $c_2(c)$, etc.] is obtained by means of a Newton-Raphson procedure[18] for a given bulk concentration c and using the boundary condition $c_{M+1}=c_M$ for some $M\gg 1$.

In practice in the (LE_1) we compare, for example, the function $c_0(c_2)$ obtained by eliminating the bulk concentration from the segregation equilibrium profile [$c_0(c)$ and $c_2(c)$] to the function $c_0(c_2)$ obtained by eliminating the time from the kinetics [$c_0(t)$ and $c_2(t)$] obtained using the KTBIM.[11,27]

Second local equilibrium representation (LE_2): In some cases, the kinetics describes a situation that does not correspond to the equilibrium segregation for any bulk concentration. It is clearly the case for the (c_k,c_{k+1}) configurations observed during the dissolution of 1 or 2 ML of Fe on Cu(110) (Sec. III B 1). However, the condition mentioned above is also fulfilled; i.e., the deposited matter quits the surface and forms these quasistationary configurations very fast compared to the time the system takes to dissolve completely the deposit. It suggests that during this configurations the deposit is in local equilibrium in a finite region (extended over M planes) close to the surface that is also in contact permanently with the rest of the volume. The configurations appearing during the kinetics must then correspond to the equilibrium ones obtained from a finite system or ''equivalent thin layer'' (ETL) of the same size M, containing the same mean concentration C_{ETL} and in contact at every time with a bulk plane having the instantaneous concentration given by the kinetics.[28]

To prove if the second representation of the local equilibrium is satisfied and represented by an ETL of M layers, we extract at every time during the dissolution kinetics the concentration of the $M+1$ plane $c_M(t)$ and the average concentration over the first M layers C_{ETL}. Using this values we solve the following coupled nonlinear system of equations:[29]

$$\frac{c_i}{1-c_i}=\frac{c_{M-1}(t)}{1-c_{M-1}(t)}\exp\left\{-\frac{\Delta H_i-\Delta H_{M-1}}{kT}\right\}, \quad i=0,M-2; \quad (12)$$

$$C_{ETL}(t)=\frac{1}{M}\sum_{i=0}^{M-1} c_i \quad (13)$$

and compare the profile obtained in this ETL with the one obtained in the dissolution kinetics.

Let us mention here that if the first representation LE_1 applies the second one LE_2 also does because both systems of equations are equivalent. The use of the LE_2 in these cases rarely gives additional information. The utility of the second representation is more useful when the kinetic profiles do not correspond to any equilibrium segregation solution of the system of equations (11), in particular when the average concentration C_{ETL} lies in the miscibility gap.

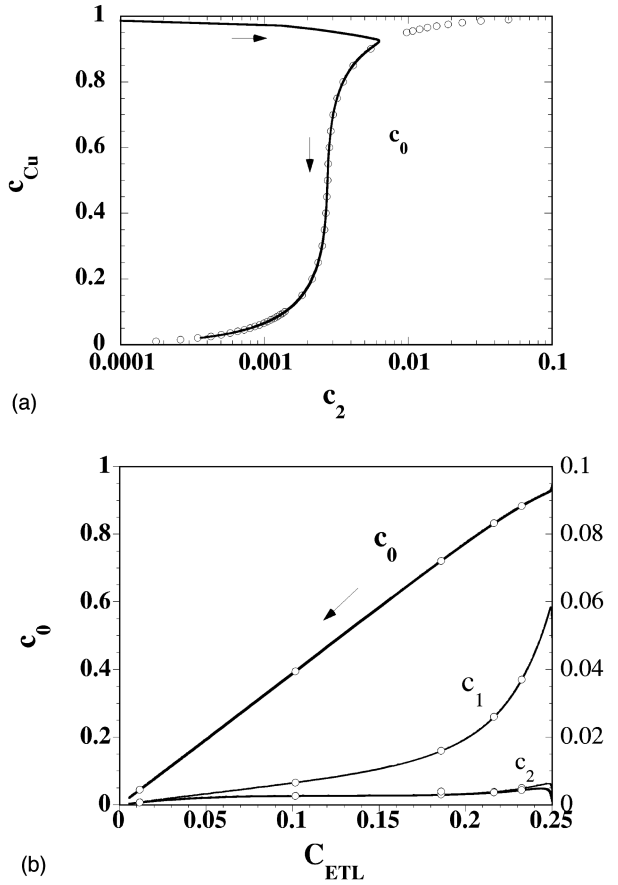

FIG. 8. Local equilibrium during the dissolution of one monolayer of Cu on Fe(110) at $T=1100$ K. (a) LE_1 representation. The surface concentration of Cu (c_0) is plotted vs the Cu concentration on the third plane (c_2). Comparison between kinetics results (solid line) and the equilibrium isotherm (circles). The arrows show the time evolution. (b) LE_2 representation. The Cu concentrations of the first four planes (c_i, $i=0,3$) are plotted vs C_{ETL}. Comparison between dissolution kinetics results (solid lines) and equilibrium solutions in an ETL of four planes (circles).

A. Cu deposited on Fe

1. 1 ML of Cu on Fe(110)

For one monolayer of Cu deposited on Fe both the LE_1 and LE_2 representations can be used to follow the kinetics near the surface. In Fig. 8(a) we show the applicability of the LE_1 representation by plotting the copper surface concentration c_0 versus the concentration of the third plane c_2. We can see that apart from the rapid variation at the beginning (c_0 going from 1 to 0.9 while c_2 going from 0 to 0.006) the local equilibrium is satisfied. It is clear from this figure that c_2 remains almost constant during the kinetics, one condition necessary to explain the $\sqrt{t}$ behavior of the surface concentration that we have mentioned in Sec. III A 1. The reason

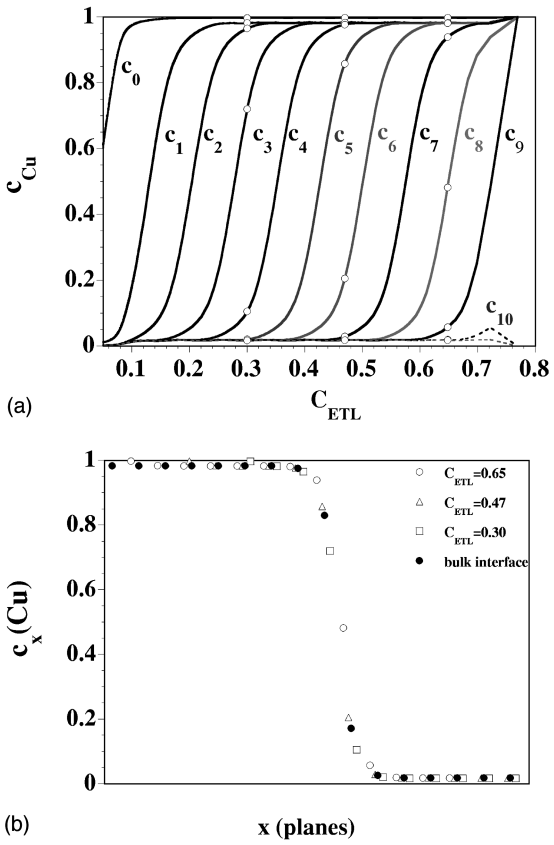

FIG. 9. Local equilibrium for the dissolution of 10 ML of Cu on Fe(110) at $T=1100$ K. (a) LE_2 representation. The Cu concentrations of the first 11 planes ($c_i, i=0,10$) are plotted vs C_{ETL}. Comparison between dissolution kinetics (solid lines) and equilibrium solutions in an ETL of 13 planes (circles). (b) Comparison between the instantaneous concentration profiles at three different times (empty markers) with the equilibrium interface profile in the bulk at equilibrium (full circles).

for that is the strong segregation responsible for a very abrupt segregation equilibrium isotherm (the surface concentration going from 0 to 1 while $c_2 \simeq 0.003$) and the validity of the local equilibrium.

In the LE_2 representation [Fig. 8(b)], we consider an ETL of four planes. The comparison between the kinetic curves (solid lines) and the concentrations obtained from this pseudo- ''thin-layer'' at five different times (empty circles) shows that the local equilibrium in this second representation is also satisfied.

2. 10 ML of Cu on Fe(110)

During the dissolution of 10 ML of Cu on Fe where the layer by layer dissolution mode takes place we can wonder what the spatial extension of the local equilibrium is. Is the interface between the deposit and the substrate included in this extension, or is the local equilibrium only restricted to the surface?

For the interface we can use the LE_2 representation, with an ETL of a number of planes greater than the size of the deposit. We show in Fig. 9(a) the concentration of the first 11 planes from the kinetic dissolution in function of the instantaneous average concentration (solid lines). We find again a constant spacing in C_{ETL} for the dissolution of each layer similar to the spacing in $\sqrt{t/t_0}$ found in Fig. 2. The reason is that from Eqs. (10) and (13), we can see that C_{ETL} has a linear dependence on $\sqrt{t/t_0}$:

$$C_{ETL} \simeq \frac{m(t)}{13} = \frac{1}{13}(10 - 2c_\alpha \sqrt{t/\pi t_0}). \tag{14}$$

The comparison of the kinetics curves with three equilibrium solutions of an ETL of thirteen planes [circles in Fig. 9(a)] shows that the local equilibrium is clearly satisfied. The region $C_{ETL} < 1/13$ concerns the dissolution of the surface layer and in this case both representations of the local equilibrium can be used. The use of the LE_1, for example, would give the same curves that we have already presented for the dissolution of 1 ML of Cu on Fe in Fig. 8(a), proving that the surface region also is in local equilibrium. The only difference is that the kinetic curves will now transverse the figure coming from the high c_2 region.

From Fig. 9(a) and also from Fig. 2 we can see that this layer by layer dissolution mode consists of a continuous displacement of an interface towards the surface. The envelope of this interface does not evolve while approaching the surface and corresponds to the equilibrium interface between two regions of limiting concentrations c_α and $1-c_\alpha$[23,30] [see Fig. 9(b)].

TABLE I. Summary of the quasistationary configurations that appear during the dissolution of 1 and 2 Fe ML on Cu(110) at 700 K and at 1100 K.

	1 ML	2 ML
700 K	(c_2, c_3)	(c_1, c_2) and (c_2, c_3)
1100 K		(c_2, c_3)

B. Fe deposited on Cu

1. 1 and 2 ML of Fe on Cu(110)

In this section we will show how the use of the LE_2 representation allows us to understand the appearance of the quasistationary configurations (c_k, c_{k+1}) summarized in Table I.

$T=700$ *K*. We will first concentrate on the dissolution of 2 ML where two quasistationary configurations exist (see Table I). To show that these configurations are well described using the local equilibrium, we show in Fig. 10(a) the LE_2 representation with and ETL of five planes. Let us note that the time evolution in this figure occurs from right to left: the maximum value of the mean concentration C_{ETL} for an ETL of M layers and a deposit of 2 ML occurs at $t=0$ and is equal to $C_{ETL}(t=0)=2/M$, the final value is $C_{ETL}(t=\infty)=0$ corresponding to the total dissolution of the deposit. It is easy to distinguish in this figure the two quasistationary configurations: the first one (c_1, c_2) that appears for $0.40 > C_{ETL} > 0.22$, and the second one (c_2, c_3) for $C_{ETL} < 0.22$. It also interesting to point out that at the beginning of the dissolution, the decrease of the surface concentration c_0 occurs at constant $C_{ETL}=0.40$, showing that the surface enrichment in copper takes place via atom exchanges between the first planes. The filled circles in Fig. 10(a) represent the

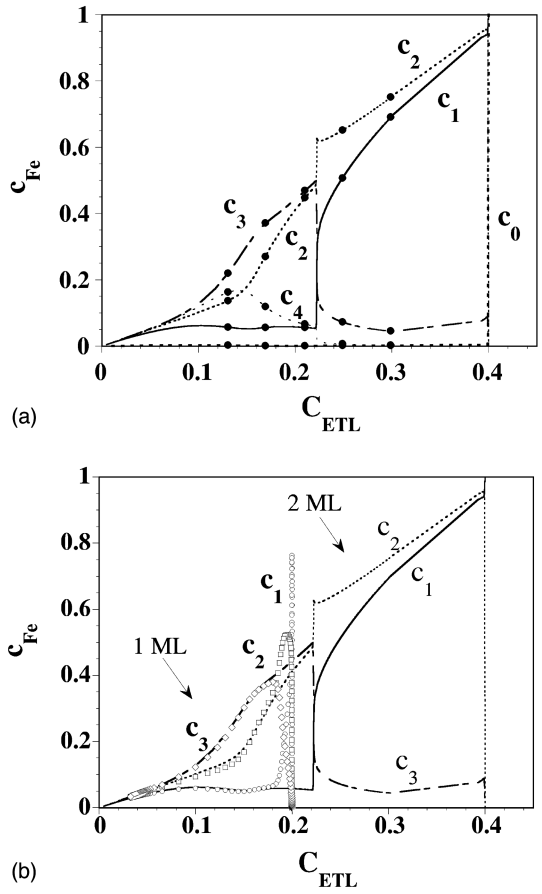

FIG. 10. LE_2 representation of the local equilibrium for the dissolution of a thin Fe deposit on Cu(110) at $T=700$ K. (a) 2 ML of Fe on Cu(110). The Fe concentrations of the first five planes (c_i, $i=0,4$) are plotted vs C_{ETL}. Comparison between dissolution kinetics (lines) and equilibrium solutions in an ETL of five planes (full circles). (b) Comparison between the dissolution kinetics of 1 (points) and 2 ML (lines) of Fe on Cu(110). The Fe concentrations of the first three sublayers planes (c_i, $i=1,3$) are plotted vs C_{ETL}.

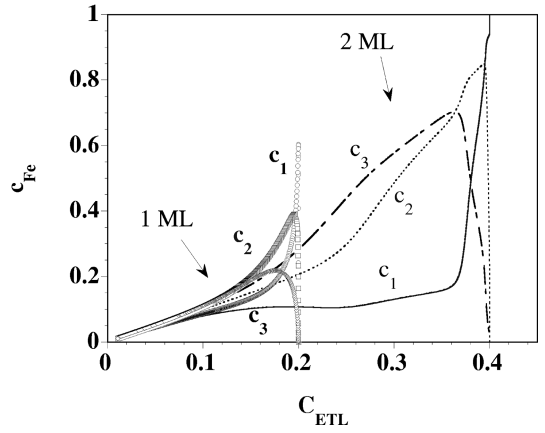

FIG. 11. LE_2 representation of the local equilibrium for the dissolution of a thin Fe deposit on Cu(110) at $T=1100$ K. Comparison between the dissolution kinetics of 1 (points) and 2 ML (lines). The kinetics concentration profiles are at local equilibrium in the whole range of concentration in a ETL of five planes. The Fe concentrations of the first three sublayers planes (c_i, $i=1,3$) are plotted vs C_{ETL}.

equilibrium profiles. They correspond perfectly to the kinetic curves in the two quasistationary configurations. Another important point is that at each average concentration, there is only one solution of the system of equations (12) and (13). Then, the transition between the quasistationary configurations corresponds, via the local equilibrium, to equilibrium phase transitions in a finite system (the equivalent thin layer).

For the dissolution of 1 ML at this temperature we have seen in Sec. III B 1 that there is only one quasistationary configuration (see Table I). The comparison between the LE_2 representation for 1 ML and 2 ML using an ETL of five layers is shown in Fig. 10(b). It is easy to understand why the (c_1,c_2) configuration does not appear in this case. The average concentration required for the existence of this configuration is at least 0.22 and for 1 ML the maximum value of the mean concentration is $C_{ETL}(t=0)=0.2$.

$T=1100$ *K.* At $T=1100$ K, there is a (c_2,c_3) configuration for the dissolution of 2 ML and no quasistationary configurations for the 1 ML case. The comparison between the LE_2 representations in these cases for an ETL of five layers is shown in Fig. 11. For 2 ML we can recognize the (c_2,c_3) configuration beginning at $C_{ETL}\simeq 0.35$ that evolves slowly to a more Fickian dissolution when the average concentration decrease below 0.25. This value is higher than the maximum average concentration for 1 ML $C_{ETL}(0)=0.2$ explaining why only the Fickian dissolution mode is seen in this case.

2. 10 ML of Fe on Cu(110)

As we have seen in Sec. III B 2, at the beginning of the kinetics, the segregation effect leads to the appearance of a floating layer of copper at the surface, the deposit being buried under the surface. Then, two different modes of layer by layer dissolution compete corresponding to the dissolution of the precipitate starting either from one extremity of the precipitate or from the other.

The copper enrichment of the surface at the beginning can be seen as a segregation kinetics, the surface copper concentration going from 0 to 1 while the copper concentration inside the Fe deposit is very low. If one represents the surface copper concentration versus the concentration in the Fe-rich region not far from the surface, one will find that the kinetics curve follows the equilibrium LE_1 representation of Fig. 8(a). The main difference with respect to the kinetic curve given in Fig. 8(a) is that in the present case the kinetic curve will follow the equilibrium also in the high-c_0 and high-c_2 values (going from the lower left corner to the upper right one). It means that during this part of the kinetics the surface is in local equilibrium.

Further in time the LE_1 representation is no longer adequate and as for the 10 ML Cu on Fe dissolution we use the LE_2 representation with a 13 planes ETL (see Fig. 12). The equilibrium profile calculated at $C_{ETL}\simeq 0.68$ is the only solution to the system of Eqs. (12) and (13) and corresponds to the stage labeled III in Fig. 7(b). At lower C_{ETL} we find two possible solutions for the equilibrium profile (circles and squares in Fig. 12), one that corresponds to the actual kinetic profile and the other to a profile that would appear if the layer by layer dissolution happened in the opposite extremity

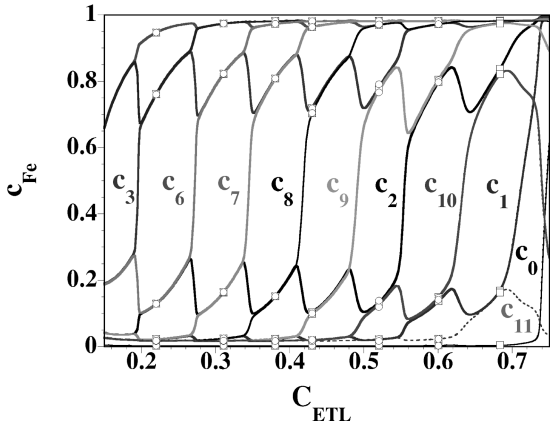

FIG. 12. Local equilibrium for the dissolution of 10 ML of Fe deposited on Cu(110) at $T=1100$ K. The Fe concentrations of the first 12 planes ($c_i, i=0,11$) are plotted vs C_{ETL}. Comparison between dissolution kinetics (solid lines) and equilibrium solutions in an ETL of 13 planes (circles and squares).

of the precipitate. Work is in progress to clarify the reasons for the occurrence of one or another mode.

V. CONCLUSION

Within an energetic and a kinetic model taking into account the phase separation tendency in the bulk and the surface segregation effects, we have studied the different dissolution modes that occur during the dissolution of thin (1 or 2 ML) and thick (10 ML) deposits of Fe on Cu and of Cu on Fe.

For Cu deposited on Fe the strong Cu surface segregation leads to the trapping of the deposit at the surface. For 1 monolayer we found a linear decrease of the surface copper concentration with $\sqrt{t}$ that can be related to the equilibrium segregation isotherm: the dissolution takes place while the surface region is in local equilibrium. In the case of a thick deposit (10 ML), a layer by layer dissolution mode takes place starting from the plane at the interface between the deposit and the substrate. The shape of this interface corresponds to the equilibrium interface between two semi-infinite phases having the bulk solubility limit concentrations (c_α and c_β), the stiffness of the interface being due to the large miscibility gap. For the 10 ML dissolution both the near surface and the interface regions are in local equilibrium.

For Fe deposited on Cu, the deposit has a higher surface energy and the substrate element climbs through the deposit to reach the surface. This leads to the formation of a copper layer or bilayer floating on the Fe-rich precipitate. For low temperatures and depending on the number of deposited monolayers, the Fe precipitate spreads essentially between two planes forming quasistationary configurations that slow down the dissolution considerably. These configurations correspond to equilibrium profiles for a finite system with the same instantaneous quantity of matter. In the case of thick deposit (10 ML Fe/Cu), the surface undergoes also a copper enrichment in the first stage of dissolution. Then a competition between two layer by layer dissolution modes takes place: the dissolution occurs either from the top or from the bottom of the precipitate. On one hand, the system tends to favor the dissolution from the top for energetic reasons. The top interface is constrained by the presence of the surface giving a small energetic preference to move the precipitate down into the bulk. On the other hand, due to the diffusion length, it is easier for the precipitate to dissolve itself from the bottom. The alternation between these two modes during kinetics depends on the deposit thickness and the temperature. Using similar mean-field and also Monte Carlo simulations, the study of the temperature influence on this competition is under progress for the NiAg system.[31] In the case of thin deposit, the Monte Carlo simulations show the formation of small clusters under the surface in contrast to the mean-field results presented here. We can wonder if this behavior would appear in the case of thick deposit, and what is the deposit critical size driving the formation of small clusters.

Finally, we want to underline the usefulness of the local equilibrium concept to understand the reasons for the slow down of the kinetics, the transitions between different quasistationary configurations, and the shape of the instantaneous interfaces.

[1] See, for example, J. Magn. Magn. Mater. **165** (1997).
[2] F. J. A. den Broeder, W. Hoving, and P. J. H. Bloemen, J. Magn. Magn. Mater. **93**, 562 (1991).
[3] Th. Detzel, M. Vonbank, M. Donath, N. Memmel, and V. Dose, J. Magn. Magn. Mater. **152**, 287 (1996).
[4] C. Gallis, B. Legrand, and G. Tréglia, Surf. Sci. **377-379**, 1033 (1997).
[5] C. Gallis, Ph.D. thesis, Université de Paris VI, 1997.
[6] D. A. Steigerwald, I. Jacob, and W. F. Egelhoff, Surf. Sci. **202**, 472 (1988).
[7] T. Detzel and N. Memmel, Phys. Rev. B **49**, 5599 (1994).
[8] H. P. Noh, Y. J. Choi, J. Y. Park, I. C. Jeong, Y. D. Suh, and Y. Kuk, J. Vac. Sci. Technol. B **14**, 1188 (1996).
[9] J. M. Roussel, A. Saúl, G. Tréglia, and B. Legrand, Phys. Rev. B **55**, 10 931 (1997).
[10] G. Tréglia, B. Legrand, and F. Ducastelle, Europhys. Lett. **7**, 575 (1988).
[11] A. Senhaji, G. Tréglia, B. Legrand, N. T. Barrett, C. Guillot, and B. Villette, Surf. Sci. **274**, 297 (1992).
[12] B. Legrand, A. Saúl, and G. Tréglia, Mater. Sci. Forum **155-156**, 165 (1994).
[13] G. Salje and M. Feller-Kniepmeier, J. Appl. Phys. **48**, 1833 (1977).
[14] In this kinetic model (the KTBIM) the atomistic mechanism of diffusion is the direct exchange of *A* and *B* atoms. However for the diffusion coefficient appearing in Eq. (1) we use the experimental one for diffusion of *A* impurities in a *B* matrix that usually corresponds to the real atomistic mechanism of diffusion by vacancies. As the diffusion coefficient does not depend on the concentration the role of *D* in our model is just to determine the time scale.
[15] M. Aldèn, H. L. Skriver, S. Mirb, and B. Johansson, Surf. Sci. **315**, 157 (1994).
[16] D. Tomanek, A. A. Aligia, and C. A. Balseiro, Phys. Rev. B **32**,

5051 (1985); G. Tréglia and B. Legrand, Phys. Rev. B **35**, 4338 (1987).
[17] P. Turchi, Ph.D. thesis, Université de Paris VI, 1984.
[18] W. H. Press, B. P. Falnnery, S. A. Teukolsky, and W. T. Vetterling, *Numerical Recipes* (Cambridge University Press, Cambridge, 1986).
[19] M. M. Eisl, B. M. Reich, and H. Störi, Appl. Surf. Sci. **70-71**, 137 (1993).
[20] A. Saúl, B. Legrand, and G. Tréglia, Phys. Rev. B **50**, 1912 (1994).
[21] J. Eugène, Ph.D. thesis, Université d'Aix Marseille III, 1989; H. Giordano, Ph.D. thesis, Université d'Aix Marseille I, 1993.
[22] A. Saúl, B. Legrand, and G. Tréglia, Surf. Sci. **307-309**, 804 (1994).
[23] A. Saúl, Mater. Sci. Forum **155-156**, 233 (1994).
[24] J. Du Plessis, Solid State Phenom. **11**, 43 (1990).
[25] M. Lagües and J. L. Domange, Surf. Sci. **47**, 77 (1975).
[26] G. Tréglia, B. Legrand, J. Eugène, B. Aufray, and F. Cabané, Phys. Rev. B **44**, 5842 (1991).
[27] A. Senhaji, Ph.D. thesis, Université de Paris-Sud (Orsay), 1993.
[28] S. Delage, B. Legrand, F. Soisson, T. Bigault, A. Saúl, and G. Tréglia, J. Phys. IV **6**, C7-151 (1996).
[29] The two systems of Eqs. (11) and (12) are in some way mathematically equivalent. The first one is directly obtained from a grand-canonical description of the segregation problem where the bulk concentration (univocally related to the chemical potential) is fixed but the total quantity of matter is unknown. The second one follows from a canonical description of the same problem in a finite system where the total quantity of matter (or the concentration average) is known.
[30] A. Saúl, B. Legrand, and G. Tréglia, Surf. Sci. **331-333**, 805 (1995).
[31] J. M. Roussel, A. Saúl, G. Tréglia, and B. Legrand (unpublished).